Identification of the Predominant Non-Native Histidine Ligand in Unfolded Cytochrome *c*†

Wilfredo Colón,‡,§ L. Paul Wakem,||,⊥ Fred Sherman,|| and Heinrich Roder*,‡,#

Institute for Cancer Research, Fox Chase Cancer Center, Philadelphia, Pennsylvania 19111, Department of Biochemistry, University of Rochester School of Medicine and Dentistry, Rochester, New York 14642, and Department of Biochemistry and Biophysics, University of Pennsylvania, Philadelphia, Pennsylvania 19104-6059

Received July 14, 1997; Revised Manuscript Received August 22, 1997⊗

ABSTRACT: The heme and its two axial ligands, His18 and Met80, play a central role in the folding/unfolding mechanism of cytochrome *c*. Because of the covalent heme attachment, His18 remains bound under typical denaturing conditions, while the more labile Met80 ligand is replaced by an alternate histidine ligand. To distinguish between the two possible non-native histidine ligands in horse cytochrome *c*, variants with a His26 to Gln or His33 to Asn substitution were prepared using a yeast expression system. Protonation of the non-native histidine ligand in the GuHCl-denatured state results in a pronounced blue shift of the Soret heme absorbance band (low-spin to high-spin transition). While substitution of His26 has no effect on the apparent pK_a of this transition (5.7 ± 0.05), the H33N variant exhibits a substantially higher pK_a (6.1 ± 0.05), indicating that His33 is the dominant sixth heme ligand in denatured cytochrome *c* and that His26 (or another nitrogenous group) acts as a ligand in the absence of a histidine at position 33. The kinetics of the pH-induced ligand dissociation shows two phases which were assigned to each of the two histidine ligands on the basis of their distinct temperature dependence. Despite their nearly identical equilibrium unfolding transitions, the two histidine mutants show differences in their folding kinetics. While the kinetic behavior of H26Q cyt *c* is very similar to that of the wild-type, the H33N mutation leads to loss of a kinetic phase with a rate in the 2−10 s^{-1} range that has previously been attributed to the rate-limiting dissociation of a trapped non-native histidine, which is thus identified as His33.

A unique feature of cytochrome *c* (cyt *c*) is the presence of a covalently bound heme group that plays an essential role in folding and function. In native horse cyt *c*, Met80 and His18 serve as axial ligands to the heme (Figure 1). However, in GuHCl-unfolded cyt *c* at neutral pH, Met80 is replaced by one of two additional histidine residues in cyt *c*, His26, or His33, while His18 remains bound to the heme (*1*−*4*). The presence of non-native histidine-heme iron ligation in unfolded cyt *c* at pH 7 creates a kinetic barrier for folding that allows the trapping of a native-like intermediate with interacting N- and C- terminal helices (*5*−*8*). This barrier manifests itself through the presence of a slow (2−10 s^{-1}, depending on conditions) folding phase, which dominates the absorbance- and fluorescence-detected kinetics at pH 7, but is significantly reduced in amplitude at pH 5, where His26 and His33 are largely protonated. Although trapping a kinetic folding intermediate with native-like features may allow detection and study of an otherwise elusive kinetic intermediate (*5*, *9*), the presence of slow rate-determining steps makes it more difficult to study the structural events at early stages of folding. Whereas the folding kinetics of cyt *c* is simplified at pH 5, non-native heme ligation cannot be prevented completely by lowering the pH since acid denaturation sets in before His26 and/or His33 are fully protonated (*10*). Recently, Pierce and Nall

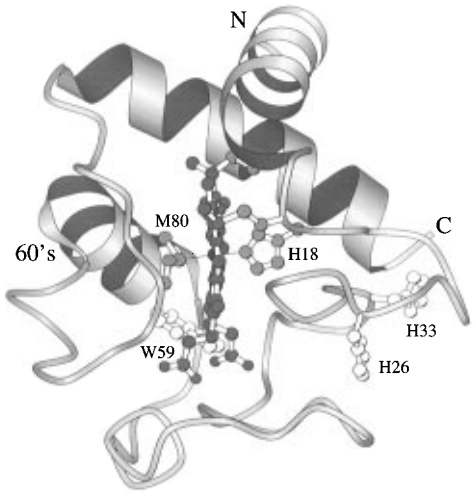

FIGURE 1: Ribbon diagram of horse cytochrome *c* based on the crystal structure (*22*). The side chains of the native heme ligands (Met80 and His18), potential non-native ligands (His26 and His33), and the single tryptophan (Trp59) are shown explicitly. The figure was prepared using the program MolScript (*31*).

† This work was supported by NIH grants GM35926 (to H.R.) and GM12702 (to F.S.) and by NIH grant CA06927 and an appropriation from the Commonwealth of Pennsylvania to the Institute for Cancer Research. W.C. was an NSF minority fellow.

* Correspondence should be addressed to this author at the Fox Chase Cancer Center. Phone: (215) 728-3123. Fax: (215) 728-3574. E-mail: H_Roder@fccc.edu.

‡ Fox Chase Cancer Center.

§ Present address: Department of Chemistry, Rensselaer Polytechnic Institute, Troy, NY 12180-3590.

|| University of Rochester.

⊥ Present address: Department of Dermatology, University of Rochester School of Medicine, Rochester, NY 14642.

University of Pennsylvania.

⊗ Abstract published in *Advance ACS Abstracts,* October 1, 1997.

[1] Abbreviations: Cyt *c*, horse cytochrome *c*; GuHCl, guanidine hydrochloride; WT, wild-type; H26Q and H33N, His to Gln substitution at position 26, and His to Asn substitution at position 33 of wild-type cytochrome *c*.

S0006-2960(97)01697-8 CCC: $14.00

(*11*) studied the folding of a double mutant of yeast iso-2 cyt *c* where His33 and His39 were mutated to Asn and Lys, respectively. They were able to show that the folding of H33N/H39K iso-2 cyt *c* is accelerated by an order of magnitude compared to the WT protein, thereby supporting the hypothesis that non-native histidine-heme ligation results in a kinetic barrier for folding. Furthermore, cyt c_2 from photosynthetic bacteria has only a single histidine that serves as the native axial ligand to the heme, and it exhibits simpler folding kinetics (*12*).

There has been little information regarding the relationship between the location of histidine residues in the amino acid sequence and their ability or preference to serve as a heme iron ligand. Since non-native heme ligation occurs when cyt *c* is unfolded by GuHCl or urea, it is likely that there are minimal structural constraints, and that binding preference will be related to the location of the histidine in the amino acid sequence. Using a competition approach, Muthukrishnan and Nall (*4*) determined the effective concentration of histidine residues in GuHCl-unfolded yeast iso-1 and iso-2, and tuna cyt *c* by titrating with imidazole, an extrinsic heme ligand. Their results demonstrated that multiple histidine residues can share the available heme iron ligation site in unfolded cyt *c* (His18 remains bound to the heme), suggesting that the intramolecular effective concentration of the individual histidine residues determines their ligation preference. On the basis of preliminary experiments with the H26Q variant of cyt c, Elöve et al. (*7*) suggested that His33 is the predominant heme ligand in unfolded cyt c, implying that structural constraints play a role in histidine ligation preference. To test this hypothesis, we have prepared two horse cyt *c* mutants, H26Q and H33N, designed to clarify the individual roles of His26 and His33 as non-native heme iron ligands in GuHCl-unfolded cyt *c*. Complementary equilibrium and stopped-flow kinetic experiments identify His33 as the dominant heme iron ligand in GuHCl-unfolded cyt *c*.

MATERIALS AND METHODS

Materials and Sample Preparation. Horse heart ferricytochrome *c* (Type VI from Sigma Chemical Co.) was used without further purification. Cytochrome *c* mutants were expressed in yeast (*13*) and purified as previously described (*9*). The gene CYC1-HORSE, encoding horse cyt c, was previously constructed with synthetic oligonucleotides, and expressed in the yeast *Saccharomyces cerevisiae* (*13*). In contrast to commercial horse heart cytochrome *c*, this recombinant protein is only ~70% acetylated at the N-terminal glycine, and approximately 80% of lysine 72 is trimethylated (*13*). Preliminary equilibrium experiments (described below) showed that the effect of these post-translational modifications on our results was negligible. Therefore, the commercial protein was used for all subsequent experiments on WT cyt *c*. The H33N (CYC1-1101) and H26Q (CYC1-1105) mutant forms were constructed by the method of Kunkel et al. (*14*), and both of the altered genes were integrated in the CYC1 region of the yeast strain B-6748 as previously described (*13*). A first attempt to construct a double mutant, H26Q/H33N, was unsuccessful; we are currently preparing this variant using a PCR-based mutagenesis approach. The sequences of these CYC1 genes were verified by amplifying the appropriate region by PCR, and subsequently sequencing the double-stranded DNA. Protein concentration was determined spectrophotometrically using an extinction coefficient for oxidized cyt *c* of 1.06×10^5 at 409 nm (*2*).

Equilibrium Fluorescence Measurements. Fluorescence measurements were performed on an Aminco-Bowman Series 2 fluorescence spectrometer (SLM-Aminco, Urbana, IL), using a 1 cm quartz cuvette thermostated at 10 °C. Excitation and emission wavelengths were 280 and 350 nm, respectively, and both slits were set to 4 nm. Solutions of folded (100 mM sodium acetate, pH 5.0) and unfolded (5−6 M GuHCl, 100 mM sodium acetate, pH 5.0) cyt *c* were prepared at concentrations of 2−4 μM. The fluorescence was measured for the native protein and cyt *c* solutions at progressively higher concentrations of GuHCl, achieved by repetitive withdrawal of native cyt *c* from the cuvette followed by addition of a corresponding volume of unfolded cyt *c* solution. The fluorescence signal of cyt *c* was normalized relative to an equimolar solution of N-acetyltryptophanamide in 6 M GuHCl and 100 mM sodium acetate, pH 5.0. The free energy of unfolding in the absence of denaturant, ΔG_{H_2O}, was obtained by nonlinear least-squares analysis of the data, based on a two-state model with a linear dependence of unfolding free energy, ΔG, on denaturant concentration, $\Delta G = \Delta G_{H_2O} - mC = m(C_m - C)$ (*15*, *16*).

Ligation Equilibrium in Unfolded Cytochrome c. The pH-induced deligation of non-native heme iron ligands in unfolded cyt *c* was monitored by measuring the Soret absorbance maximum with a Perkin-Elmer λ 4B UV−vis spectrophotometer. The pH of an unfolded solution of cyt *c* (50 mM sodium phosphate, 4.5 M GuHCl, pH 8.0) was gradually decreased by adding a small amount (5−10 μL) of 1 N HCl. A gradual change in Soret maximum to lower wavelength indicative of a change in heme ligation state was observed. Most experiments were done at room temperature. No difference was observed between experiments at 10 and 25 °C. The maximum in Soret absorbance (λ_{max}) was plotted against pH to obtain curves that were fitted by nonlinear least-squares analysis to the equation

$$\lambda_{max}(\mathrm{pH}) = [\lambda_{max}(\mathrm{pH\ 9}) - \lambda_{max}(\mathrm{pH\ 4})]/[10^{n(\mathrm{pH}-\mathrm{p}K_a)} + 1] + \lambda_{max}(\mathrm{pH\ 4}) \quad (1)$$

where *n* is the number of protons involved in the transition and pK_a is the pH at the midpoint of the transition.

Optically Detected Stopped-Flow Measurements. Kinetic experiments were performed on a Bio-Logic SFM-4/QS stopped-flow instrument (Molecular Kinetics, Pullman, WA) equipped with a 0.8×0.8 mm^2 cuvette. The dead-time was determined to be in the range 1.3−1.8 ms (depending on the flow rate used). A 150 W Xe/Hg arc lamp and monochromator (0.5 mm slit widths) were used for excitation at 280 nm, and a high-pass glass filter with 324 nm cutoff (No. 51255, Oriel Corp., Stratford, CT) was used for measuring the tryptophan fluorescence emission. Heme absorbance changes were monitored using a tungsten lamp (LS-10, Hi-Tech) and a 0.5 nm band width. The signal changes from 64 μs to ~100 s were recorded in a single kinetic trace, using a previously described logarithmic averaging method (*17*).

The kinetics of ligand dissociation under unfolding conditions were monitored by absorbance at 411 nm, after a rapid

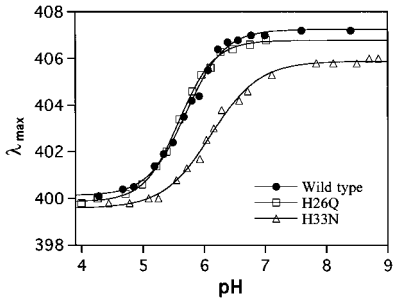

FIGURE 2: Comparison of the pH-induced shift in the Soret absorbance maximum of WT, H26Q, and H33N cyt *c*. The pH was decreased by adding small volumes of 1 N HCl to unfolded solutions of the cyt *c* variants (5−10 μM) in 4.5 M GuHCl, 50 mM phosphate buffer, pH 7.5−8.5. All experiments were carried out at room temperature.

Table 1: Acid Titration of GuHCl-Denatured Cyt *c*[a]

cyt *c*	pK_a	*n*
WT[b]	5.71 ± 0.05	1.38 ± 0.09
WT[c]	5.61 ± 0.03	1.20 ± 0.1
H26Q	5.60 ± 0.05	1.50 ± 0.06
H33N	6.11 ± 0.05	1.10 ± 0.08

[a] The pK_a and *n* values were obtained by nonlinear least-squares analysis of the data using eq 1. [b] Horse heart cyt *c* from Sigma. [c] Recombinant WT horse cyt *c* expressed in yeast.

pH jump. The pH jumps were achieved by mixing 1 part of unfolded oxidized cyt *c* (100 μM, 4.5 M GuHCl, 50 mM phosphate) at pH 7.8 with 5 parts of acetate buffer (100 mM, 4.5 M GuHCl) at pH 4.6 to obtain a final pH 4.8−5.0. All kinetic experiments were performed at 10 °C.

The folding kinetics of cyt *c* were measured at 10 °C following a 6-fold dilution of an unfolded solution of cyt *c* in 4.2 M GuHCl (100 mM acetate, pH 5.0) to various final GuHCl concentrations within and below the unfolding transition region. Final protein concentrations were 10−30 μM. The individual amplitude of the observable kinetic phases was internally normalized with respect to the total observable fluorescence change. The amplitude of unresolved processes occurring in the dead-time (burst-phase), which accounts for ~65% of the total fluorescence change, both for WT cyt *c* (*9*) and the two histidine mutants studied here (data not shown), was not included in the analysis.

RESULTS AND DISCUSSION

pH-Dependent Histidine Ligation Equilibrium. The Soret absorbance band of cyt *c* is very sensitive to ligation and spin state (*18, 19*). GuHCl- or urea- unfolded oxidized cyt *c* has a maximum Soret absorbance at 407 nm and lacks a 620 nm band, which is characteristics of a low-spin iron containing two strong-field axial ligands (*1*). A decrease in the pH of a GuHCl-unfolded cyt *c* solution induces a shift in the Soret absorbance maximum from 407 to 400 nm, consistent with the loss of a strong-field ligand coupled with the protonation of a side-chain nitrogen. Figure 2 shows the result of the pH titration curves for GuHCl-unfolded WT cyt *c* and the H26Q and H33N variants. WT cyt *c* (including both commercial preparations and recombinant horse cyt *c* expressed in yeast) and the H26Q variant exhibit similar titration curves (pK_a = 5.6−5.7, n = 1.2−1.5; Table 1), whereas the behavior of H33N is quite distinct (pK_a = 6.1, n = 1.1). The similarity of the pH-dependent ligand equilibrium between the WT and H26Q (Figure 2, Table 1) indicates that His26 does not participate significantly in non-native heme ligation in the presence of histidine at position 33. On the other hand, mutation of His33 to Asn causes a significant shift in the low-spin to high-spin transition toward higher pH. The equilibrium data in Figure 2, thus, indicate that His33 is the predominant sixth ligand in WT and H26Q cyt *c* (above pH 5.7), while in the absence of a histidine at position 33, His26 or another unidentified side chain can serve as an alternative ligand (above pH 6.1). The observation of *n* values greater than 1 in WT (1.38) and H26Q (1.50) is consistent with an equilibrium involving two or more partially coupled ionizations. In contrast, *n* is closer to 1 in H33N (1.10), indicating an equilibrium dominated by one ionizable group. Thus, the effect of histidine mutations on the pH-induced ligand dissociation are fully consistent with His33 being the predominant non-native ligand in GuHCl-unfolded WT cyt *c*, at least near neutral pH.

Table 2: Activation Parameters for Deligation of Non-Native Histidine Ligand[a]

	fast phase		slow phase	
cyt *c*	E_a (kcal/mol)	log *A* (s^{-1})	E_a (kcal/mol)	log *A* (s^{-1})
WT	12.3 ± 0.2	11.5 ± 0.2	17.1 ± 0.7	14.6 ± 0.5
H26Q			16.8 ± 1.7	14.6 ± 1.3
H33N	12.1 ± 1.3	11.3 ± 1.0	7.8 ± 1.6	7.6 ± 1.2

[a] Activation energies, *E*a, and pre-exponential factors, *A*, describing the temperature dependence of the kinetics of ligand dissociation in the GuHCl-denatured state of WT cyt *c* and the two histidine variants.

Tsong (*3*) previously reported a pK_a of 5.1 for WT horse cyt *c* in 6 M GuHCl, which is significantly lower than that obtained in this study (Table 1). The higher GuHCl concentration used in the earlier work is probably not important, since we measured very similar titration curves at 4.5 and 6 M GuHCl. However, the discrepancy may be related to the fact that Tsong (*3*) did his experiments in the absence of buffer, whereas we used 50 mM sodium phosphate, or it may be due to pH electrode artifacts. Fortunately, this discrepancy does not affect any of our conclusions, since they are based on the comparison of WT and mutant proteins under identical experimental conditions.

Kinetics of pH-Induced Histidine Deligation. The heme-histidine deligation rate can be determined by optical methods following rapid acidification of a solution of unfolded cyt *c*. Previous stopped-flow kinetic experiments with WT cyt *c* showed biphasic behavior, suggesting that both His26 and His33 can serve as ligands to the heme iron (*7*). Furthermore, in a preliminary pH jump experiment, Elöve et al. (*7*) found that the H26Q variant of horse cyt *c* exhibits a single exponential phase, suggesting that one of the two phases seen for the WT may be due to His26.

To confirm this tentative assignment, we performed a series of pH jump experiments at several temperatures ranging from 10−30 °C to determine the activation energy of histidine deligation for the H26Q and H33N variants. Figure 3 shows the temperature dependence of the histidine deligation rates and the corresponding amplitudes for WT, H26Q, and H33N cyt *c*; Table 2 lists the corresponding activation energy (E_a) and pre-exponential factor (*A*) for the various deligation processes. Two kinetic phases are observed for the WT protein (Figure 3A); the slower phase

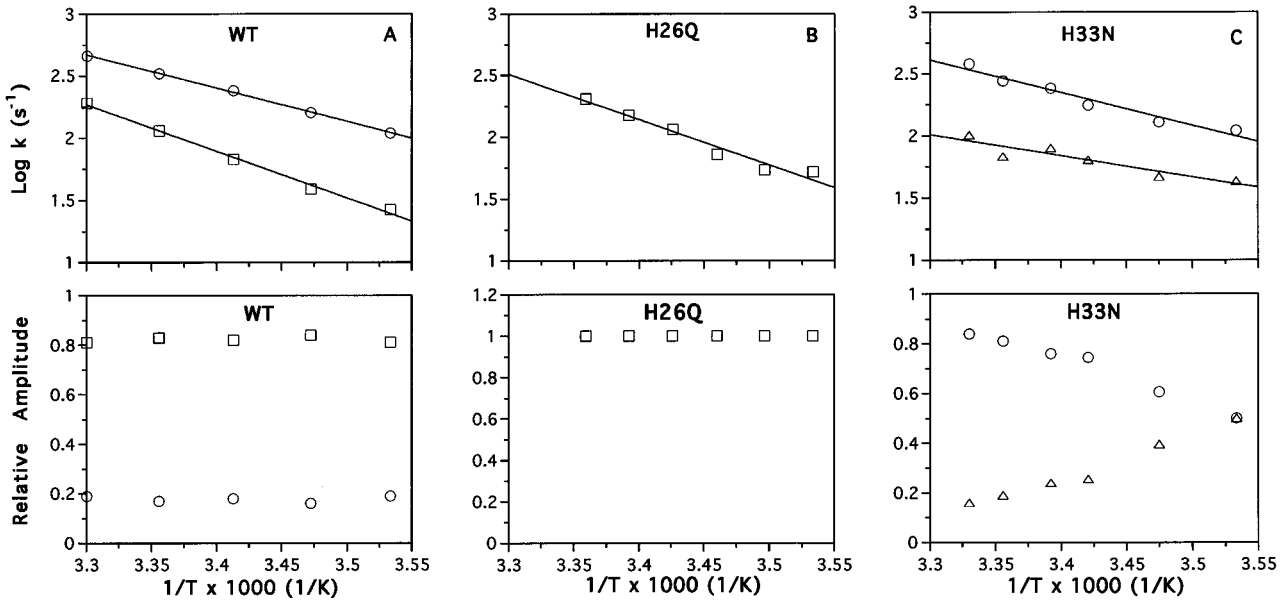

FIGURE 3: Stopped-flow kinetics of the pH-dependent heme absorbance changes at 410 nm of unfolded cyt *c* (4.5 M GuHCl and 50 mM phosphate, pH 7.8). The reaction was induced by a rapid pH jump from 7.8 to 4.6. In the upper panels (A−C) the log of the observed rate(s) is plotted as a function of the inverse absolute temperature (Arrhenius plot). The lower panels show the relative amplitudes associated with the observed kinetic phase(s). The corresponding activation energies and pre-exponential factors are listed in Table 2.

accounts for 80% of the amplitude and has an E_a of 17 kcal/mol, while the faster phase accounts for the remaining 20% of the amplitude and has an E_a of 12 kcal/mol. Figure 3B shows that the deligation kinetics for H26Q cyt *c* is a single-exponential process with a rate and activation energy closely matching the slower phase observed for the WT (Table 2). The disappearance of the faster phase in the H26Q data (Figure 3B) suggests that this minor (∼20% amplitude) phase is due to His26 deligation, and that the slower and major phase (∼80% amplitude) in the WT data (Figure 3A) can be attributed to His33 deligation. The faster His26 dissociation rate and smaller E_a indicate a lower affinity for the iron. On the basis of this observation, one would expect the slow kinetic phase observed for WT and H26Q to be absent in H33N. Although the kinetic behavior seen for H33N cyt *c* is complicated by the presence of an additional phase not seen for the other two variants, closer inspection of Figure 3C and Table 2 shows that this is indeed the case. The slower phase (E_a = 17 kcal/mol), which dominated the kinetics of WT cyt *c* (80% of the amplitude), is absent in the case of H33N, confirming its assignment to His33. Instead, the kinetics of H33N is dominated by a fast phase that closely matches the minor fast phase of WT cyt *c* at all temperatures (E_a and *A* in Table 2 are within error). Thus, His26 becomes the predominant sixth heme ligand in the variant lacking His33. However, the observation of an additional phase in Figure 3C with a lower activation energy (8 kcal/mol) than that of the histidine related processes (Table 2) suggests the involvement of at least one additional ligand other than His26 and 33. This process is most pronounced at low temperature, where the two phases of H33N cyt *c* have comparable amplitudes (Figure 3C), but its amplitude decreases as the temperature is raised, reflecting a change in the equilibrium population of heme ligand. At this time, the identity of the ligand responsible for the slower phase of H33N is unknown. Possible candidates are the N-terminal NH_2 group which is only partially acetylated in these recombinant proteins (*13*), or an NH_2 group from a deprotonated lysine side chain.

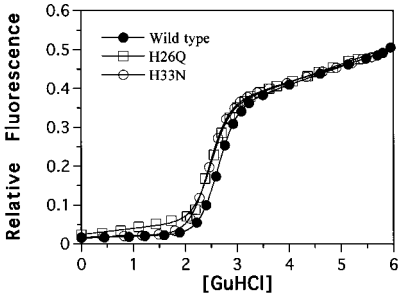

FIGURE 4: Fluorescence-detected GuHCl denaturation transitions for WT, H26Q, and H33N cyt *c* at 10 °C in 0.1 M sodium acetate, pH 5.0. The tryptophan fluorescence emission at 350 nm was normalized relative to an equimolar solution of *N*-acetyl-L-tryptophanamide.

Refolding Kinetics of Cyt c at pH 5. Because of its relatively slow rate of dissociation, a non-native histidine ligand can become trapped during folding and give rise to slow rate-limiting steps in refolding experiments (*7*, *8*). While this effect is greater at pH 7.0 where histidine side chains are largely deprotonated, it is still observable even at pH 5 or below (*7*, *10*, *20*). To study the individual involvement of His26 and His33 in folding, we measured the folding kinetics of H26Q and H33N at pH 5.0.

For a meaningful comparison of the refolding kinetics of WT with H26Q and H33N as a function of GuHCl concentration, it is important to compare their stabilities to GuHCl denaturation. The reversible GuHCl-induced unfolding transition of cyt *c* (WT, H26Q, and H33N) was monitored using tryptophan fluorescence as a probe of conformational changes. Figure 4 compares the denaturation transition for the WT, H26Q, and H33N cyt *c* variants. The equilibrium two-state thermodynamic parameters listed in Table 3 show that all three proteins are very similar in stability. The two histidine variants have slightly lower C_m values than WT, but the corresponding differences in ΔG_{H_2O} are nearly within error. While His33 is quite variable among eukaryotic cyt *c*, His26 is more highly conserved (*21*). The imidazole group of His26 forms two hydrogen bonds in cyt *c*, one with the

Table 3: Stability of Horse Cytcochrome *c* Mutants[a]

	C_m (M)	m (kcal M^{-1} mol^{-1})	ΔG_{H_2O} (kcal mol^{-1})
WT	2.61 ± 0.01	3.1 ± 0.1	8.1 ± 0.3
H26Q	2.54 ± 0.01	3.1 ± 0.1	7.9 ± 0.3
H33N	2.44 ± 0.01	3.0 ± 0.1	7.3 ± 0.2

[a] All measurements were performed at 10 °C. Cyt *c* solutions contained 0.1 M sodium acetate, pH 5.0. Equilibrium transition curves were calculated by nonlinear least-squares analysis as described in Materials and Methods. The slopes and intercepts of the pre- and post-transition baselines were used as fitting parameters, in addition to C_m and m.

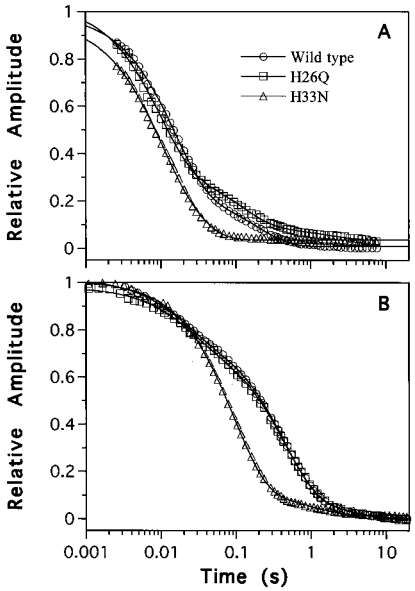

FIGURE 5: Representative stopped-flow kinetic traces for the refolding of WT, H26Q, and H33N cyt *c*. Refolding was induced by dilution of unfolded cyt *c* from 4.5 M to 1.0 M GuHCl at pH 5.0 (A) or 7.0 (B), and monitored by tryptophan fluorescence (>320 nm). The curves represent nonlinear least-squares exponential fits. The data were normalized internally with respect to the total observed amplitude.

backbone carbonyl of Pro44 that bridges two loops (residues 26−31 and residues 41−47), and one with the backbone amide of Asn31 (*22*). Therefore, the observation of similar stabilities for WT and H26Q suggests that the important hydrogen bond with Pro44 has been preserved in the H26Q variant. This is consistent with the finding of Qin et al. (*23*) that replacement of His26 by Val in rat cyt *c* destabilized the protein by almost 4 kcal/mol.

The refolding kinetics of cyt *c* was measured after rapid dilution of GuHCl-unfolded cyt *c* with buffer. Figure 5 shows representative refolding kinetic traces of WT, H26Q, and H33N cyt *c* (in 1.0 M GuHCl) at pH 5.0 (Figure 5A) and pH 7.0 (Figure 5B). The WT protein and the H26Q variant exhibit two major phases under both conditions, a faster phase with a rate of ∼100 s^{-1} at pH 5 (∼50 s^{-1} at pH 7) and a slower phase with a rate of ∼8 s^{-1} at pH 5 (∼2 s^{-1} at pH 7). At pH 5.0, the faster and slower phases account for ∼75 and 25% of the amplitude, respectively, while at pH 7.0 this ratio is inverted. The slower phase has previously been attributed to dissociation of a non-native histidine ligand in a partially folded state (*6*−8), which has recently been observed also for yeast iso-2 cyt *c* (*11*). The decrease in the relative amplitude of the slower phase at pH 5.0 (from 75 to 25%) is consistent with a decrease in the population of misligated protein in the unfolded state at pH 5.0. In the case of H33N, there are two major phases at pH 5.0 with rates of ∼140 and ∼40 s^{-1}, respectively; however, the slower phase seen for WT and H26Q is not present. At pH 7.0, the folding kinetics of H33N is essentially single exponential with a rate of ∼11 s^{-1} accounting for ∼90% of the observable amplitude. The nearly 10-fold decrease in the rate of the dominant folding phase for H33N at pH 7.0, compared to pH 5.0, is consistent with our equilibrium (Figure 2) and kinetic (Figure 3) ligand dissociation experiments, which show evidence for non-native ligation in GuHCl-unfolded H33N at pH 7.0. Figure 3 suggests that His26 serves as the major non-native ligand in the absence of His33. In fact, the refolding rate of H33N at pH 7.0 is 4.5 times faster than the slow phase for WT and H26Q (Figure 5B), consistent with the deligation rate of His26 being ∼4 times faster than that of His33 (Figure 3).

Figure 6 depicts the folding rates (on a log scale) and the corresponding amplitudes as a function of final GuHCl concentration for the three cyt *c* variants studied. The data for WT and H26Q cyt *c* are very similar; both exhibit two major refolding phases as described above. At higher GuHCl concentration, the slower phase accounts for most of the observed amplitude, while at lower GuHCl concentration, the faster phase dominates. The negligible effect of His26 suggests that His33 dominates as the non-native ligand, making the presence of His26 insignificant when His33 is present, in agreement with all previous data (Figures 2 and 3). The slower folding phase previously attributed to histidine deligation is not observed for H33N. It is interesting that His26 alone does not result in slow rate-limiting folding steps despite its ability to bind the iron in the unfolded state; this is perhaps due to its faster dissociation rate, which makes it less likely to be trapped during folding.

Some heterogeneity of the fast phase is observed in the case of WT and H33N; an additional phase with a rate of 160−260 s^{-1} appears at low GuHCl concentration, and despite the fact that this phase is only 3−4 times faster than the second phase (50−80 s^{-1}), inclusion of an additional exponential results in a significantly better fit of the kinetic data. This heterogeneity of the fast phase is not observed in H26Q, suggesting that it may be related to the presence of His26. Nevertheless, the observation that the refolding kinetics of cyt *c* is simplified by the H33N mutation while remaining almost the same in H26Q is further evidence that His33 is the predominant non-native heme iron ligand of GuHCl-unfolded cyt *c*.

Comparison of the refolding kinetic data in Figure 6 clearly shows that at pH 5.0 the refolding kinetics of cyt *c* is still coupled with deligation events, consistent with previous observations (*7, 8, 10*). For example, refolding of cyt *c* from pH 2.4 to 4.9 still results in ∼30% of slow folding species (*24*). Recently, Yeh et al. (*10*) were able to show by using resonance Raman scattering in conjunction with sub-millisecond kinetics that, even at pH 4.5, 30% of the heme iron in GuHCl-unfolded cyt *c* exists in the bis(histidine) form. When the methionine ligation site is blocked with an extrinsic ligand such as imidazole, the slow folding phase disappears completely (*7, 25*) and the refolding kinetics at pH 5 and pH 7 become identical (W. Colón, and H. Roder, manuscript in preparation). Consistent with these observations, H33N shows no evidence of slow rate-limiting steps in folding at pH 5, indicating that ligand-related complications are minimized in this cyt *c* variant. Thus, the H33N variant

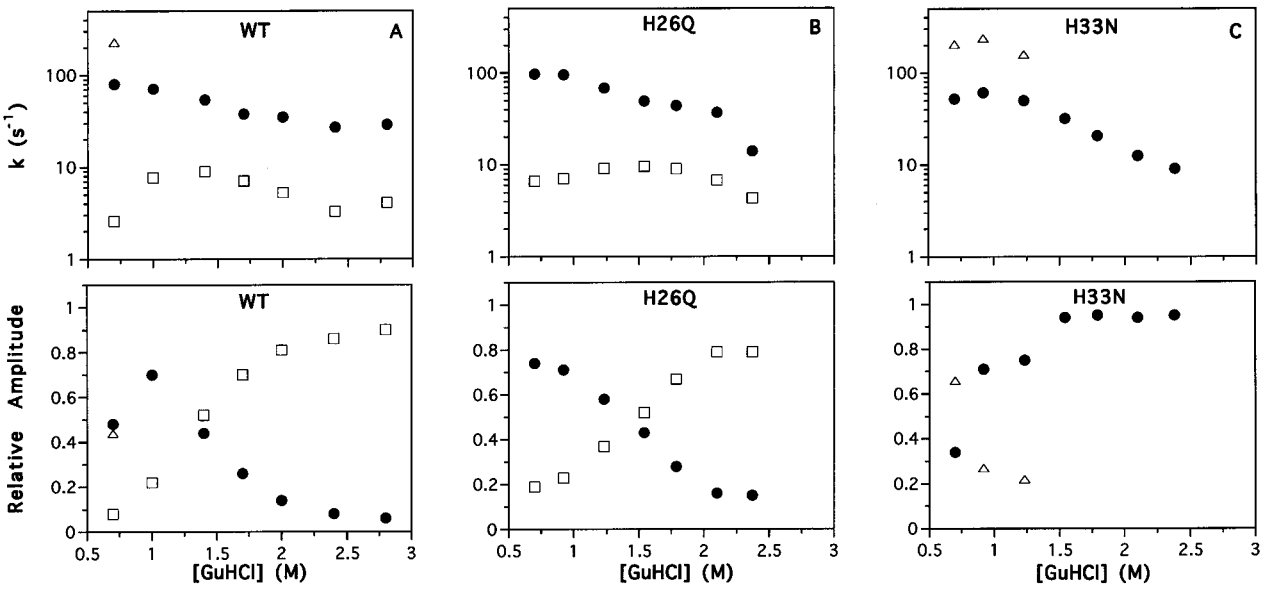

FIGURE 6: Denaturant dependence of the refolding rates and amplitudes of WT (A), H26Q (B), and H33N (C). Refolding was triggered by diluting unfolded cyt *c* solutions from 4.5 M GuHCl to various final concentrations at pH 5.0 (10 °C). The upper and lower panels show the GuHCl dependance of the folding rates and amplitudes, respectively, using matching symbols. The amplitudes were internally normalized relative to the total observable amplitude.

makes it possible to focus on the underlying structural process in the folding of cyt *c* without the complications arising from non-native heme ligation.

General Discussion. We have shown that His33 is the predominant non-native heme iron ligand in GuHCl-unfolded cyt *c*, based on three different experiments: (i) the pH-dependent ligation equilibrium, (ii) the kinetics of ligand dissociation in the denatured state, and (iii) the kinetics of refolding at pH 5. The reasons for the predominance of His33 over His26 as a non-native ligand are not fully understood, although steric and entropic factors are likely to be involved. Since Cys17 and His18 are covalently bound to the heme, His26 may not be far enough down the polypeptide chain to access the available heme ligation site opposite to His18 without some unfavorable steric interactions (for an extended chain, the distance from His18 to His26 would be ~29 Å, but excluded volume effects and chain stiffness may oppose loop formation). In contrast, His33 and His18 are 15 residues apart (corresponding to a distance of ~54 Å in an extended chain), providing seven additional residues to close the loop. Alternatively, there could be some stabilizing interactions in GuHCl-unfolded H33N cyt *c* not present in GuHCl-unfolded H26Q. This appears unlikely since one would expect a similar *m* value (which is indicative of the difference in exposed surface area between the native and unfolded state) for the equilibrium denaturation of WT and H26Q, and a different *m* value for H33N, and this is not the case (Table 3). Pierce and Nall (*11*) recently observed a marked increase in *m* value for a double mutant (H33N/H39K) of yeast iso-2 cyt *c*, compared to WT, suggesting that elimination of non-native cross-links results in a more expanded denatured state. On the other hand, Godbole and Bowler (*26*) reported a decrease in *m* values for the analogous yeast iso-1-cyt *c* variant lacking non-native histidines, indicating that the situation is more complex.

An interesting question raised by these experiments concerns the nature of the additional ligand in the case of H33N. Likely candidates are some of the 19 lysine residues present in cyt *c*. In particular, lysines 5, 7, and 8 at the N-terminal are in close proximity to the heme, even in the denatured state, and should have a high effective concentration. The pK_a of 6.1 for the deligation of the heme iron ligand (Figure 2) is significantly lower than that of lysine (~10.5), corresponding to an energetic cost of 5.5 kcal/mol, which may be more than compensated by the binding of a strong ligand to the heme iron. Another potential heme ligand is the amino-terminal NH_2 group in the fraction of recombinant cyt *c* with nonacetylated N-terminus; while cyt *c* isolated from horse is 100% N-acetylated, this level drops to 70% for the recombinant form expressed in yeast (*13*). It is possible that the 30% population with free amino-terminus may form a bond between the deprotonated NH_2 group and the heme iron. In fact, there is precedent for this type of ligation in cytochrome *f* from plant chloroplast (*27*), where the native axial heme ligand is the N-terminal amino group of Tyr 1. Also, Godbole and Bowler (*26*) recently observed that in a triple mutant (H26N/H33N/H39Q) of yeast iso-1-cyt *c* lacking all the potential non-native histidine ligands, the N-terminal amino group binds to the heme iron in the unfolded state. However, our observation that WT cyt *c* from horse heart (100% N-acetylated) and recombinant WT cyt *c* (70% N-acetylated) show, within error, identical pH titration curves (Table 1), suggests that this is not a major contribution in the case of the horse protein. Future experiments with a double histidine mutant (H26Q/H33N) of horse cyt *c* will be directed toward elucidating the nature of these potential heme ligand(s). His/Lys complexes can potentially be identified by electron paramagnetic resonance (EPR) in conjunction with near infrared magnetic circular dichroism (NIR-MCD; refs 28 and 29). Hawkins et al. (*30*) recently used this method to describe a His/His complex in a mutant of yeast iso-1-cyt *c*.

In summary, we have used cyt *c* mutants with substitutions at His26 or His33 to identify the predominant non-native heme iron ligand of GuHCl-unfolded oxidized cyt *c*. Our results strongly suggest that His33 is the predominant ligand accounting for over 80% of the population of non-native

ligand. Surprisingly, we have also observed that in the absence of His33, some other intramolecular ligand, which remains to be identified, is able to bind to the heme iron and can compete with His26.

ACKNOWLEDGMENT

We thank L. Comfort for synthesizing the oligonucleotides, G. A. Elöve and A. Khorram for preliminary experiments, and S.-H. Park, J. M. Sauder, M. C. R. Shastry, and W. F. Walkenhorst for helpful comments.

REFERENCES

1. Babul, J., and Stellwagen, E. (1971) *Biopolymers 10*, 2359−2361.
2. Babul, J., and Stellwagen, E. (1972) *Biochemistry 11*, 1195−1200.
3. Tsong, T. Y. (1975) *Biochemistry 14*, 1542−1547.
4. Muthukrishnan, K., and Nall, B. T. (1991) *Biochemistry 30*, 4706−4710.
5. Roder, H., Elöve, G. A., and Englander, S. W. (1988) *Nature 335*, 700−704.
6. Elöve, G. A., and Roder, H. (1991) *ACS Symp. Ser. 470*, 50−63.
7. Elöve, G. A., Bhuyan, A. K., and Roder, H. (1994) *Biochemistry 33*, 6925−6935.
8. Sosnick, T. R., Mayne, L., Hiller, R., and Englander, S. W. (1994) *Nat. Struct. Biol. 1*, 149−156.
9. Colón, W., Elöve, G. A., Wakem, L. P., Sherman, F., and Roder, H. (1996) *Biochemistry 35*, 5538−5549.
10. Yeh, S.-R., Takahashi, S., Fan, B., and Rousseau, D. L. (1997) *Nat. Struct. Biol. 4*, 51−56.
11. Pierce, M. M., and Nall, B. T. (1997) *Protein Sci. 6*, 618−627.
12. Sauder, J. M., MacKenzie, N. E., and Roder, H. (1996) *Biochemistry 35*, 16852−16862.
13. Hickey, D. R., Jayaraman, K., Goodhue, C. T., Shah, J., Fingar, S. A., Clements, J. M., Hosokawa, Y., Tsunasawa, S., and Sherman, F. (1991) *Gene 105*, 73−81.
14. Kunkel, T. A., Roberts, J. D., and Zakour, R. A. (1987) *Methods Enzymol. 154*, 367−383.
15. Pace, C. N. (1986) *Methods Enzymol. 131*, 266−280.
16. Santoro, M. M., and Bolen, D. W. (1992) *Biochemistry 31*, 4901−4907.
17. Khorasanizadeh, S., Peters, I. D., Butt, T. R., and Roder, H. (1993) *Biochemistry 32*, 7054−7063.
18. Ikai, A., Fish, W. W., and Tanford, C. (1973) *J. Mol. Biol. 73*, 165−184.
19. Brems, D. N., and Stellwagen, E. (1983) *J. Biol. Chem. 258*, 3655−3660.
20. Takahashi, S., Yeh, S.-R., Das, T. K., Chan, C.-K., Gottfried, D. S., and Rousseau, D. L. (1997) *Nat. Struct. Biol. 4*, 44−50.
21. Moore, G. R., and Pettigrew, G. W. (1990) *Cytochrome c: evolutionary, structural and physiochemical aspects*, Springer-Verlag, Berlin.
22. Bushnell, G. W., Louie, G. V., and Brayer, G. D. (1990) *J. Mol. Biol. 214*, 585−595.
23. Qin, W., Sanishvili, R., Plotkin, B., Schejter, A., and Margoliash, E. (1995) *Biochim. Biophys. Acta 1252*, 87−94.
24. Sosnick, T. R., Mayne, L., and Englander, S. W. (1996) *Proteins 24*, 413−426.
25. Chan, C.-K., Hu, Y., Takahashi, S., Rousseau, D. L., Eaton, W. A., and Hofrichter, J. (1997) *Proc. Natl. Acad. Sci. U.S.A. 94*, 1779−1784.
26. Godbole, S., and Bowler, B. E. (1997) *J. Mol. Biol. 268*, 816−821.
27. Martinez, S., Huang, D., Szczepaniak, A., Cramer, W., and Smith, J. (1994) *Structure 2*, 95−105.
28. Gadsby, P. M. A., and Thomson, A. J. (1990) *J. Am. Chem. Soc. 112*, 5003−5011.
29. Cheesman, M. R., Greenwood, C., and Thomson, A. J. (1991) *Adv. Inorg. Chem. 36*, 201−255.
30. Hawkins, B. K., Hilgen-Willis, S., Pielak, G. J., and Dawson, J. H. (1994) *J. Amer. Chem. Soc. 116*, 3111−3112.
31. Kraulis, P. J. (1991) *J. Appl. Crystallogr. 24*, 946−950.

BI971697C